Abstract

Chapter 1

Introduction

1.1 Introduction

Chapter 2

Methodology

A finite element model is used to represent a area(2D) of an intragranular space. The 2D mesh is created using Trimesh. Two material objects are created, one being U-10Mo and another one is Xenon. Thermal conductivity of U-10Mo is used from Burkes et. al [2]. Different set of thermal conductivity of Xenon is used. The effective thermal conductivity of

2.1 Introduction

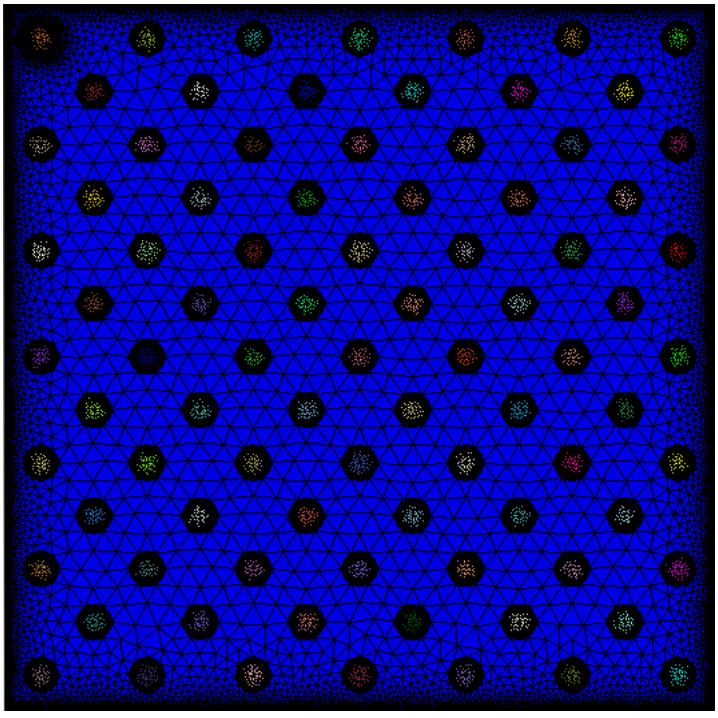

Figure 2.1: Meshed Xenon bubble inside U-10Mo matrix

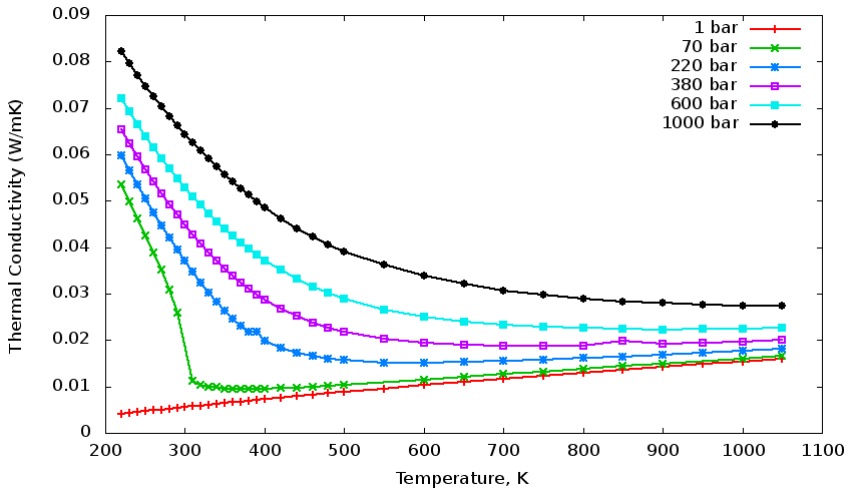

Figure 2.2: Thermal Conductivity of Xenon with increasing pressure

Chapter 3

Results

3.1 Results

In this study, heat conduction simulations were used to study the impact of overall heat transfer coefficient in the presence of Xenon bubble in the intragranular region. Grain boundary resistance and the influence of intergranular fission is not included in this calculation. This simulation is design to see the impact on heat transfer due to the formation of Gas Bubble Superlattice. Bubble superlattice formation inside U-Mo fuel stabilizes the fuel swelling behavior but heavily impacts the heat transfer capability [1]. This might be due to Xenon's very low thermal conductivity. Thermal properties of Xenon was also considered in this work. Xenon's thermal conductivity is function of both temperature and pressure [6]. Since the size of the bubble changes with the burnup and fission density, thermal conductivity of the bubble also changes [5]. Pressure inside the bubble is highly depend on the curvature of the bubble. The reults is plotted in figure 3.1. As it can be seen from the plot that thermal conductivity of U-10Mo drops with the presence of the Xenon bubble. And with the increase of the Xenon bubble's size it also decreases the. The result is also compared with Maxwell-Eucken equation [4] and with Hashin and Strikman [3]. In figure 3.2 the comparison is showed.

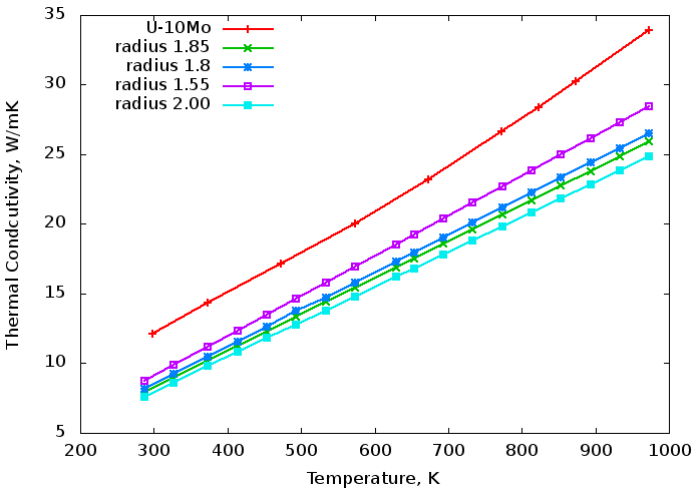

Figure 3.1: Comparison between the thermal conductivity of U-10Mo and the inclusion of Xe bubble of different sizes

FEM calculations were performed on 2.1 in order to calculate the thermal flux and the thermal conductivity in 2D. Since thermal conductivity of Xenon is a function of both temperature and pressure, six different pressure has been chosen to represend the conductivity (Figure 2.2). Eventhough the dependence of thermal conductivity is evident, the results show no change in the overall thermal conductivity in the fuel. Pressure in the bubble is significantly higher than the 1000 bar in some situation [7]. The increased pressure inside the bubble creates another probability of having phase change from gas to solid [8].

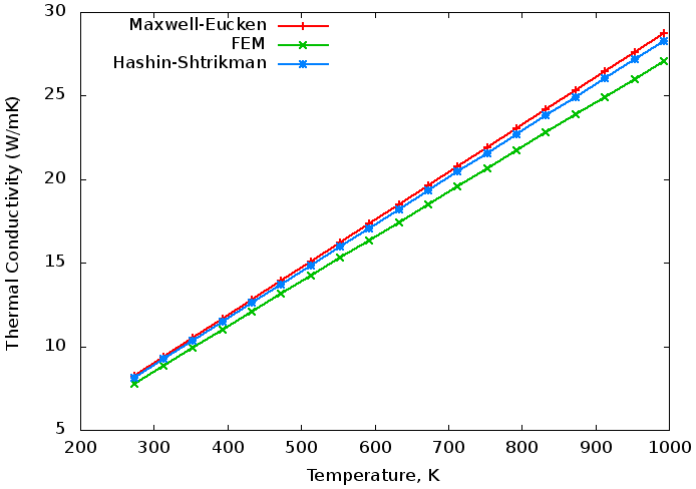

Figure 3.2: Comparison of predicted thermal conductivity of U-10Mo with Xenon bubble against the Maxwell-Eucken and Hashin and Shtrikman

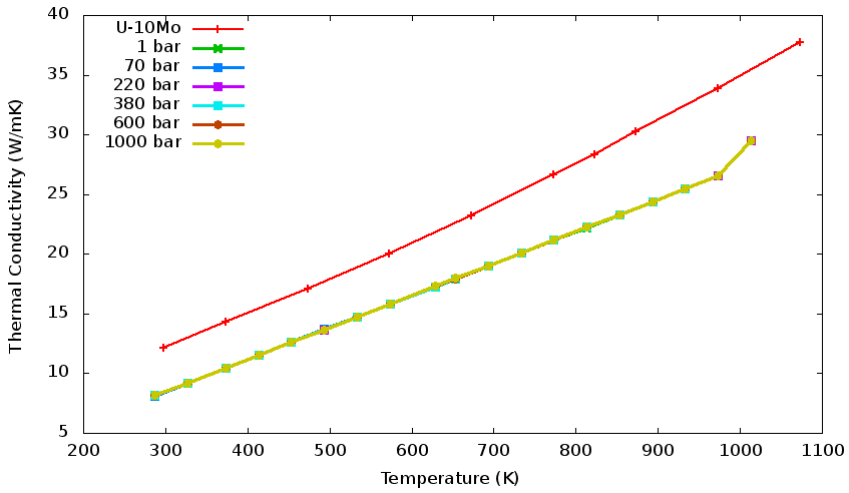

Figure 3.3: Over all thermal conductivity U-10Mo using thermal conductivity of Xenon of several pressure

Chapter 4

Discussions and conclusions

Chapter 5

Acknowledgments

Bibliography

[1] Douglas E Burkes et al. "Thermal properties of U–Mo alloys irradiated to moderate burnup and power". In: *Journal of Nuclear Materials* 464 (2015), pp. 331–341.

[2] Douglas E Burkes et al. "Thermo-physical properties of DU–10wt.% Mo alloys". In: *Journal of Nuclear Materials* 403.1 (2010), pp. 160–166.

[3] Zvi Hashin and Shmuel Shtrikman. "A variational approach to the theory of the effective magnetic permeability of multiphase materials". In: *Journal of applied Physics* 33.10 (1962), pp. 3125–3131.

[4] James Clerk Maxwell. *A treatise on electricity and magnetism*. Vol. 1. Clarendon press, 1904, p. 440.

[5] Brandon D Miller et al. "Advantages and disadvantages of using a focused ion beam to prepare TEM samples from irradiated U–10Mo monolithic nuclear fuel". In: *Journal of Nuclear Materials* 424.1 (2012), pp. 38–42.

[6] Viktor Abramovich Rabinovich et al. "Thermophysical properties of neon, argon, krypton, and xenon". In: (1987).

[7] Hongxing Xiao et al. "Atomistic simulations of the small xenon bubble behavior in U–Mo alloy". In: *Materials & Design* 74 (2015), pp. 55–60.

[8] J Zheng et al. "Thermodynamics, compressibility, and phase diagram: Shock compression of supercritical fluid xenon". In: *The Journal of chemical physics* 141.12 (2014), p. 124201.

Appendix A

XYZ Algorithm

```
clc
clear all
NN=input('Input the value of N');
%------next 13 lines assign an index IG to each basis function
C=zeros(3,3,3,3);
IG=0;
for I=1:3
    for L=1:NN+1
        for M=1:NN+1
            for N=1:NN+1
             if (L+M+N > NN+3), break, end
             IG=IG+1;
             IC(IG)=1;
             LB(IG)=1;
             MB(IG)=1;
             NB(IG)=1;

            end
        end
    end

end
rank=0.5*(NN+1)*(NN+2)*(NN+3);
NR=IG;
Gamma=zeros(rank,rank);
for IG=1:NR
     for JG=IG:NR
         I=IC(IG);
         J=IC(JG);
         LS=LB(IG)+LB(JG);
         MS=MB(IG)+MB(JG);
         NS=NB(IG)+NB(JG);

         Gamma(IG,JG)=C(I,1,J,1)*LB(IG)*LB(JG)*func(LS-2,MS,NS)+...
```

```
        C(I,2,J,2)*MB(IG)*MB(JG)*func(LS,MS-2,NS)+...
        C(I,3,J,3)*NB(IG)*NB(JG)*func(LS,MS,NS-2)+...
        C(I,1,J,2)*LB(IG)*MB(JG)+...
        C(I,2,J,1)*MB(IG)*LB(JG)*func(LS-1,MS-1,NS)+...
        C(I,1,J,3)*LB(IG)*NB(JG)+...
        C(I,3,J,1)*NB(IG)*LB(IG)*func(LS-1,MS,NS-1)+...
        C(I,2,J,3)*MB(JG)*NB(IG)+...
        C(I,3,J,2)*NB(IG)*MB(JG)*func(LS,MS-1,NS-1);
    Gamma(JG,IG)=Gamma(IG,JG);
  if(I==J) E(IG,IG)=func(LS,MS,NS) ;
    end
end
end


[vects vals]=eig(E\Gamma);
```